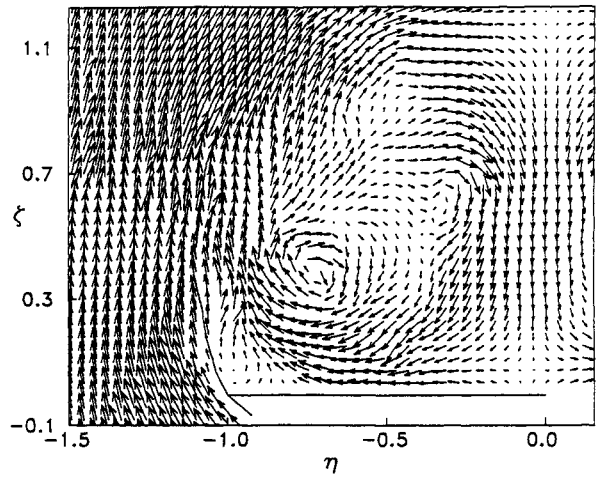

Fig. 4a Instantaneous crossflow velocity field at α = 45 deg: pitch-up from α_i = 25 deg to α_f = 50 deg, ξ = 0.79, and Å = 0.025. Vector density 1/4th actual.

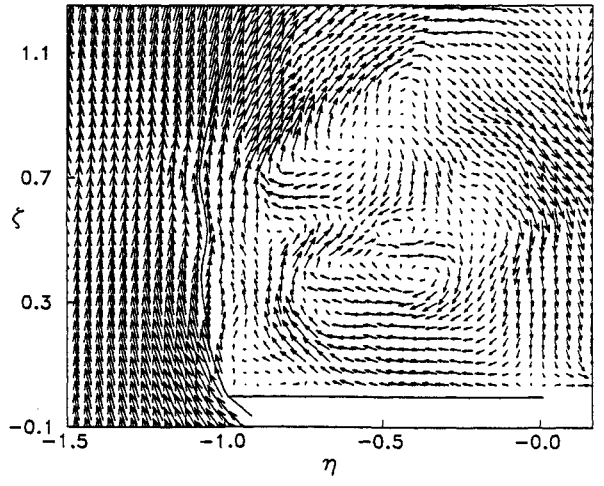

Fig. 4b Instantaneous crossflow velocity field at α = 45 deg: pitch-down from α_i = 50 deg to α_f = 25 deg, ξ = 0.79, and Å = 0.025. Vector density 1/4th actual.

This preservation of the vortex structure correlates well with the location of instantaneous vortex breakdown. As shown by Magness,[9] with a geometrically similar delta wing in a pitch-up maneuver from α_i = 30 deg to α_f = 55 deg at Å = 0.15, the location of vortex breakdown at α = 45 deg is downstream of the trailing edge ($\xi > 1.0$) in contrast to its location at ξ = 0.22 for the stationary wing. For the present pitch-up case at α = 45 deg, the implication is that vortex breakdown has not moved upstream of the ξ = 0.79 location as a direct result of the dynamic motion.

Furthermore, irrespective of whether the vortex is highly coherent (Figs. 3a and 4a) or essentially nonexistent (Figs. 3b and 4b), the locus of the separation streamline implies that, in the instantaneous sense, no flow is entrained into the leading-edge vortex.[13] It therefore appears that the vorticity feeding the vortex originates from leading-edge separation at upstream locations during these pitching maneuvers.

In summary, by application of the PIV technique, it is possible to identify the instantaneous nature of both the coherent vortical structure and the structure of regions of gross stall on a pitching delta wing. The occurrence of these extreme classes of flow structure is linked to the dynamic hysteresis of vortex breakdown location on the wing. Existence of a stall region can result in large outward displacement of the instantaneous separation streamline at the cross section of observation. In cases where the coherent structure of the vortex is preserved, it is not necessary for the feeding sheet to exhibit an inward-spiralling motion.

Acknowledgment

The authors appreciate the support of the Air Force Office of Scientific Research.

References

[1]Wolffelt, K. W., "Investigation of the Movement of Vortex Burst Position with Dynamically Changing Angle of Attack for a Schematic Delta Wing in a Water Tunnel with Correlation to Similar Studies in Wind Tunnels," AGARD CPP-413, 1986.

[2]Rockwell, D. O., Atta, R., Kuo, C. H., Hefele, C., Magness, C., and Utsch, T., "On Unsteady Flow Structure from Swept Edges Subjected to Controlled Motion," *Proceedings of the Second Workshop on Unsteady Separated Flow*, U.S. Air Force Systems Command, Frank J. Seiler Research Lab. Rept. FJSRL-TR-88-0004, Sept. 1988, pp. 299–312.

[3]Atta, R., and Rockwell, D., "Leading-Edge Vortices Due to Low Reynolds Number Flow Past a Pitching Delta Wing," *AIAA Journal*, Vol. 28, June 1990, pp. 995–1004.

[4]Reynolds, G. A., and Abtahi, A. A., "Instabilities in Leading-Edge Vortex Development," AIAA Paper 87-2424, 1987.

[5]Magness, C., Robinson, O., and Rockwell, D., "Control of Leading-Edge Vortices on a Delta Wing," AIAA Paper 89-0999, 1989.

[6]Gad-el-Hak, M., and Ho, C. M., "The Pitching Delta Wing," *AIAA Journal*, Vol. 23, Nov. 1985, pp. 1660–1665.

[7]Ashley, H., Katz, J., Jarrah, M. A. M., and Vaneck, T., "Unsteady Aerodynamic Loading of Delta Wings for Low and High Angles of Attack," *International Symposium on Nonsteady Fluid Dynamics*, edited by J. A. Miller and D. P. Telionis, Vol. 92, ASME Fluids Engineering Div., 1990, pp. 61–78.

[8]Adrian, R. J., "An Image Shifting Technique to Resolve Directional Ambiguity in Double-Pulsed Laser Velocimetry," *Applied Optics*, Vol. 25, 1986, pp. 3855–3858.

[9]Magness, C., "Unsteady Response of the Leading-Edge Vortices on a Pitching Delta Wing," Ph.D. Dissertation, Lehigh Univ., Bethlehem, PA, 1991.

[10]Meynart, R., "Instantaneous Velocity Field Measurements in Unsteady Gas Flow by Speckle Velocimetry," *Applied Optics*, Vol. 22, 1983, pp. 535–540.

[11]Lourenco, L., Krothapalli, A., Buchlin, J. M., and Riethmuller, M. L., "A Noninvasive Experimental Technique for the Measurement of Unsteady Velocity and Vorticity Fields," *Aerodynamic and Related Hydrodynamic Studies Using Water Facilities*, AGARD CPP-413, June 1987, p. 23.

[12]Landreth, C. C., and Adrian, R. J., "Measurement and Refinement of Velocity Data Using High Image Density Analysis in Particle Image Velocimetry," *Applications of Laser Anemometry to Fluid Mechanics: Proceedings of the 4th International Symposium*, ASME, Springer-Verlag, New York, 1989, pp. 484–497.

[13]Magness, C., Robinson, O., and Rockwell, D. "Flow Structure on a Pitching Delta Wing." *Bulletin of American Physical Society*, 1990, Abstract KE5, page 2335.

Time-Average Loading on a Two-Dimensional Airfoil in Large Amplitude Motion

G. M. Graham* and M. Islam†
Ohio University, Athens, Ohio 45701

Introduction

REFERENCE 1 describes the results of an analytical study of the performance of a hypothetical dynamically "aug-

Presented as Paper 90-2810 at the AIAA Atmospheric Flight Mechanics Conference, Portland, OR, Aug. 20–22, 1990; received Nov. 24, 1990; revision received April 29, 1991; accepted for publication April 29, 1991. Copyright © 1991 by the American Institute of Aeronautics and Astronautics, Inc. All rights reserved.

*Assistant Professor, Mechanical Engineering Department. Member AIAA.

†Research Assistant.

mented lift vehicle" (ALV). To produce the dynamic augmentation in lift, the ALV wings were uncoupled from the fuselage so that the wings could be mechanically pitched while, at the same time, the vehicle body could be maintained at a minimum drag trim. The ALV airfoil motion history was essentially a ramp up to a high angle of attack followed almost immediately by a ramp down to the original angle of attack. The study assumed that the wings of the ALV could be reduced in size (due to the dynamic increase in lift) and the design criterion was that the ALV wings should produce the same total lift as the wings of a conventional vehicle (CV) of similar design. The ALV and CV wings were taken to be NACA 0015 airfoils and the following relationship for wings of finite span was used to size the ALV wings:

$$\frac{A_L C_{L_{max}} q S_{ALV}}{(1 + m_0/\pi \mathrm{AR}_{ALV})} = \frac{0.8 C_{L_{max}} q S_{CV}}{(1 + m_0/\pi \mathrm{AR}_{CV})} \quad (1)$$

where $C_{L_{max}}$ is the maximum steady-state section lift, q is the reference pressure, S is the planform area, m_0 is section lift-curved slope, and AR is the aspect ratio. The constant of 0.8 on the right side is due to the fact that the CV used only 80% of the maximum static lift. On the left side the term A_L is a parameter that quantifies the dynamic augmentation in lift and is defined as the ratio of the time-average section lift over the combined ramp-up and -down motions to the maximum steady-state section lift. Reference 1 presents NACA 0015 dynamic section lift data for which the maximum time-average lift yielded $A_L = 1.114$. However, the existence of higher values of A_L was presupposed and the ALV mission analysis was carried out using a value of $A_L = 1.5$. The results showed a near 20% increase in straight-and-level range over the CV and improved range and maneuverability for a terrain-following mission. This note presents NACA 0015 dynamic section lift data at conditions for which time-average lift values of $A_L = 1.5$ and above were measured.

Experiment

Tests were conducted using a 6-in. chord NACA 0015 airfoil in a tow tank. The tank has a width of 12 ft, a length of 30 ft, and a depth of 4 ft. The airfoil was supported vertically and the clearance between the free end and the bottom of the tank was 1 in. The airfoil translational velocity was 2.03 ft/s which gives a Reynolds number of 10^5. The airfoil was pitched about the quarter chord. The pitch was imparted using a 3-hp stepper motor which is interfaced to an IBM p.c. controller. The normal and axial forces acting on the airfoil were measured using strain gauges mounted on the drive shaft which connects the airfoil to the stepper motor. The gauges were arranged in two separate bridges, each bridge sensitive to the desired force only. The angle of attack was measured using a precision rotational potentiometer fixed to the airfoil drive shaft. The lift and drag forces were computed from the normal and axial force data and the angle of attack data. The strain gauge signals were low-pass filtered at a cutoff frequency of 150 Hz and the data sampling rate was 300 Hz per signal. The axial load measurements were also filtered using a digital notch filter tuned to the natural frequency of the towing structure which was determined to be near 4 Hz. Large vibrations did not occur in the normal direction and, as such, the normal force signal was not digitally filtered. A more detailed description of data acquisition and reductions is given in Ref. 2.

Steady-state tests were conducted initially to determine the static section lift curve for the present airfoil. These data indicated that the static stall angle of attack was 15 deg and that the maximum lift coefficient prior to stall was 1.22. The unsteady motion considered in this study is shown in Fig. 1. The airfoil moves initially at a low angle of attack, α_0, and

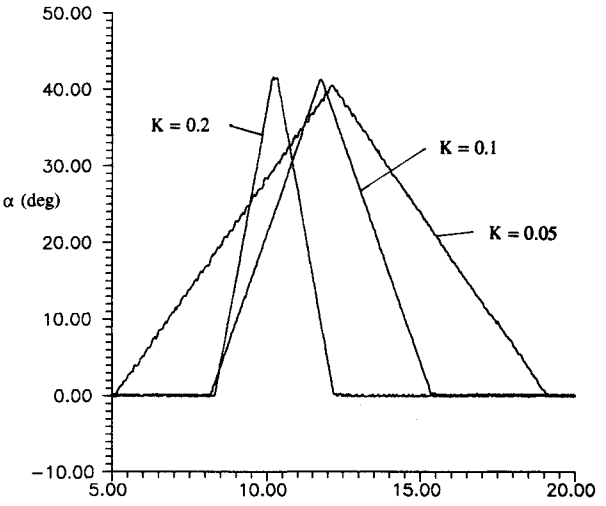

Fig. 1 Airfoil test motion.

Table 1 Test conditions

K	α_0, deg	α_{max}, deg
0.05	0	15, 20, 25, 30, 35, 40
	10	20, 25, 30, 35
0.1	0	15, 20, 25, 30, 35, 40, 45, 50, 55, 60, 65
	10	20, 25, 30, 35, 40, 45, 50, 55
0.2	0	15, 20, 25, 30, 35, 40, 45, 50, 55, 60, 65

then undergoes a ramp-up motion to a large angle of attack, α_{max}, followed by a ramp-down motion at the same pitch rate. Three pitch rates of $K = 0.05$, 0.1, and 0.2 were considered where $K = \dot{\alpha}C/2U_\infty$. Figure 1 shows present angle of attack data vs chords of travel for the cases where $\alpha_0 = 0$ deg and $\alpha_{max} = 40$ deg. Other values of α_0 and α_{max} were considered as shown in Table 1. The three pitch rates were selected to investigate slightly higher pitching rates than those reported in Ref. 1, the idea being that increasing the pitch rate may increase the time-average lift.

Results and Conclusions

Shown in Fig. 2a are representative lift coefficient results plotted as a function of angle of attack for a pitch rate of $K = 0.1$ and an initial angle of 0 deg. Arrows on the load history curves indicate the direction of pitch. Figure 2a gives some indication of the effect of α_{max} on the relative contributions of the lift during ramp up and that during ramp down to the total (ramp up and down) time-average lift. For the ramp up to $\alpha_{max} = 60$ deg, the lift begins to decrease at an angle of attack near 45 deg. Dynamic stall inception data[3] indicate that at a pitch rate of $K = 0.1$, large-scale flow separation occurs during ramp up at an angle of attack near 40 deg. The data of Fig. 2a indicate that most of the dynamic augmentation in lift occurs before flow separation and increases only slightly beyond this point. Consequently, the time-average lift during pull-up displays the same behavior. The lift force data during the ramp-down motion indicate that for large values of α_{max} the lift forces are significantly reduced below their ramp-up counterparts. A significant reduction in the lift during ramp down as α_{max} increased beyond the dynamic stall threshold was also observed for $K = 0.05$ and 0.2. The reduction of the lift during ramp down appears then to be due to the flow separation and the accompanying loss of suction pressure. The flow separation also appears to be related to the occurence of negative lift coefficients during the ramp down from large α_{max} as in the data for $\alpha_{max} = 60$ deg for angles of attack near

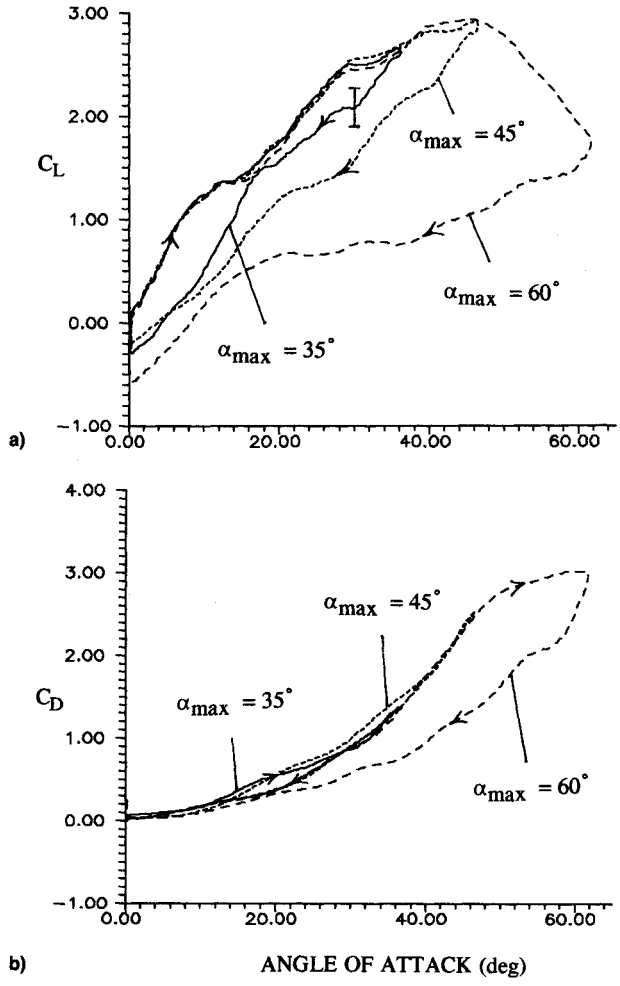

Fig. 2 Representative lift and drag coefficient data for $K = 0.1$ and $\alpha_0 = 0$ deg.

10 deg and below. Negative lift coefficients have also been reported in Ref. 1. As α_{max} is reduced into the range 30 deg $< \alpha_{max} <$ 40 deg, the lift forces during ramp down approach the ramp-up lift values and, as pointed out in Ref. 1, this suggests that the flow remains, to some extent, "contour" following.

Unsteady airfoils may also experience a dynamic augmentation in drag due primarily to augmented normal force loading. Figure 2b indicates that for values of α_{max} near the dynamic stall onset angle, the drag loading during ramp up and ramp down is nearly the same. This further suggests that the flow remains contour following. For α_{max} well beyond the stall limit, the drag during ramp down is significantly less than that for ramp up.

The time-average lift has been defined in this study as

$$C_{L_{avg}} = \frac{1}{\tau_2 - \tau_1} \int_{\tau_1}^{\tau_2} C_L(\xi)\, d\xi \qquad (2)$$

where ξ is time. The dynamic augmentation parameter A_L in Eq. (1) is given by

$$A_L = C_{L_{avg}}/C_{L_{max}} \qquad (3)$$

where for the present airfoil $C_{L_{max}} = 1.22$. In Fig. 3a, the time-average lift over the ramp-up interval of the motion is plotted as a function of α_{max}. Data at $K = 0.05$ and 0.1 for which the onset angle was 10 deg are also shown. In Eq. (2), τ_1 is the time at which the ramp up begins and τ_2 is the time when the airfoil reaches α_{max}. At each pitch rate the average lift initially increases rapidly with α_{max} and then levels out at high α_{max}. For the data at $K = 0.1$ and 0.2 there appears little to be gained by increasing α_{max} above 45 deg. Increasing the onset angle to 10 deg increases the time-average lift significantly; however, examination of the load histories, such as those in Fig. 2, indicates that this is mainly a numerical effect and not some further dynamic lift augmentation.

The time-average lift for the ramp-down motion is shown in Fig. 3b. Here, τ_1 in Eq. (2) is the time when the ramp down begins and τ_2 is the time when the airfoil returns at α_0. The lift initially increases with α_{max}, achieves a maximum at an intermediate α_{max}, and then decreases rapidly. Dynamic stall inception data[3] indicate that for ramp-up motion at low Mach numbers, a NACA 0015 airfoil will experience large-scale flow separation during ramp-up motion at the approximate angles of attack indicated by the arrows in Fig. 3b for each pitch rate. For values of α_{max} beyond the dynamic stall threshold, the average lift during ramp down decreases rapidly. As shown below, this decline in sustained lift during ramp down limits the total time-average lift for maneuvers to large α_{max}.

The effect of α_{max} on the total time-average lift is shown in Fig. 3c. Insofar as the total average lift is concerned, there is little or no advantage in increasing α_{max} beyond the dynamic stall angle of attack. A comparison of Fig. 3a, 3b, and 3c

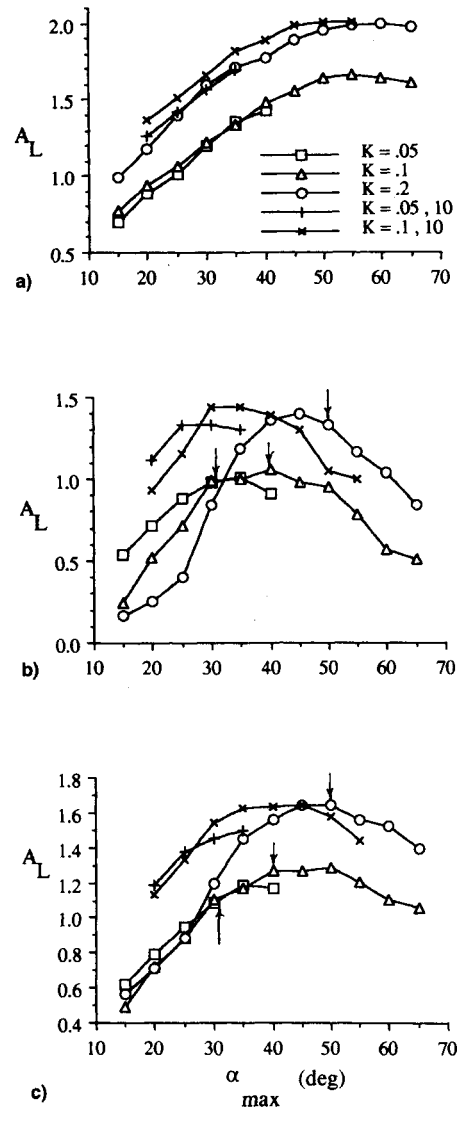

Fig. 3 Time-average lift parameter results.

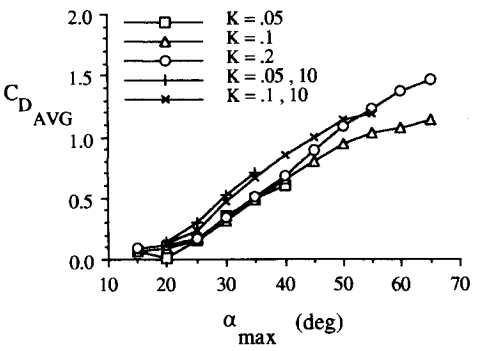

Fig. 4 Time-average drag coefficient results.

shows the average lift during the ramp-down motion is the dominant factor in the decline of the total average lift at high α_{max}. In the analysis in Ref. 1 a dynamic lift augmentation of $A_L = 1.5$ was assumed, and this resulted in an ALV with a near 20% improvement in straight-and-level range over the conventional baseline vehicle. In Fig. 3c, an augmentation of $A_L = 1.5$ was achieved at the highest pitch rate of $K = 0.2$ and $\alpha_0 = 0$ deg and for both cases of $K = 0.05$ and 0.1 for starting angles of $\alpha_0 = 10$ deg. The asssumption of Ref. 1 concerning the existence of augmentation parameters near 1.5 and above would appear then to have some justification.

Any benefits that might be gained from augmented lift must be weighed against the penalty levied by the increase in dynamic drag loading. Figure 4 shows the total time-average drag coefficients for each test motion. Figure 4 clearly shows that decreasing α_{max} is advantageous from the standpoint of average drag reduction. From Fig. 3c at the pitch rates of $K = 0.05$ and 0.1 and starting angles of 10 deg, a value of $\alpha_{max} = 35$ deg results in nearly optimum lift augmentation with respective A_L values of 1.5 and 1.63. The corresponding average drag coefficient is seen in Fig. 4 to be near 0.7, which by some standards is large. Notice, however, that the average drag decreases rapidly with decreasing α_{max}, and for $\alpha_{max} = 25$ deg and pitch rates of $K = 0.05$ and 0.1, the average drag coefficient has dropped to 0.3 and 0.24, respectively. At the same time, the lift augmentation remains well above unity and, from Fig. 3c, has values of 1.38 and 1.34, respectively. Thus for the rate of $K = 0.1$, decreasing α_{max} from 35 to 25 deg results in a drop in the average lift of 18% (though still maintaining significant lift augmentation), whereas the average drag decreases over 60%.

In the present study the pitch rate for the ramp-up and ramp-down motions was the same. For a stopping angle of $\alpha_{max} = 25$ deg the data of Fig. 3a indicate that the average lift during ramp up generally increases with pitch rate, whereas in Fig. 3b the average lift during ramp down decreases with pitch rate. There may then be some advantage in ramping up at a high rate followed by ramping down at a lower rate. In the motions studied in Ref. 1 the rate during pull-up was lower than that for pitch-down. Maintaining acceptable drag loading may be a limiting condition for defining airfoil motions for the purpose of utilizing augmented lift.

Acknowledgment

This work was supported by AFOSR Grant 87-0312.

References

[1]Jumper, E. J., Dardis III, W. J., and Stephen, E. J., "Toward an Unsteady-Flow Airplane," AIAA Paper 88-0752, Jan. 1988.

[2]Islam, M., "Experimental Study of Nonlinear Indicial Responses for a 2D NACA 0015 Airfoil," Masters Thesis, Ohio Univ., June 1991.

[3]Strickland, J. H., and Graham, G. M., "Dynamic Stall Inception Correlation for Airfoils Undergoing Constant Pitch Rate Motions," *AIAA Journal*, Vol. 24, April 1985, pp. 678–680.

Optimum Cruise Lift Coefficient in Initial Design of Jet Aircraft

Rodrigo Martinez-Val* and Emilio Perez†
Universidad Politecnica de Madrid, 28040 Madrid, Spain

Nomenclature

A = aspect ratio of wing
a = speed of sound at flight altitude
C = specific fuel consumption
C_D = drag coefficient
C_{Do} = parasite drag coefficient
C_L = lift coefficient
C_0 = parameter of specific fuel consumption in Eq. (10)
C_1 = parameter of specific fuel consumption in Eq. (10)
D = drag, $0.5\gamma pM^2SC_D$
K = range parameter
L = lift, $0.5\gamma pM^2SC_L$
M = Mach number
p = pressure at flight altitude
R = range
S = wing area
V = true cruise speed
W = airplane weight
β = exponent in the dependence of C with M
γ = ratio of specific heats of air
θ = temperature at flight altitude relative to sea level
ϕ = induced drag efficiency factor

Subscripts
cr = conditions at maximum range parameter
opt = conditions at maximum L/D

Superscripts
$*$ = condition of reference

Introduction

A VERY important point in the initial design of transport aircraft is the linkage between aerodynamic and propulsive parameters involved in the determination of the range. An airplane must be designed to fly in the surroundings of an appropriate optimum cruise condition, where fuel consumption is minimized, because of the economic impact of fuel cost in airplane operation,[1-3] and for the possibility of reducing in parallel the maximum takeoff weight, thus reaching the best design.[3,4]

In the classical analytical approach, the optimum cruise of a jet aircraft is usually considered with some simplifications, like no compressibility effects, constant specific fuel consumption,[5,6] and the constant altitude constraint imposed by air traffic control.[7,8]

Several attempts have been done to improve the former model and obtain a more realistic representation, providing complex empirical[1,7] or analytical relations[9]; most of them are not adequate for initial design.

In the present study, the specific fuel consumption is influenced by the Mach number, according to a potential law

Received July 23, 1990; revision received March 1, 1991; accepted for publication May 27, 1991. Copyright © 1991 by the American Institute of Aeronautics and Astronautics, Inc. All rights reserved.

*Professor of Aircraft Design, Department Vehiculos Aeroespaciales, Escuela Tecnica Superior de Ingenieros Aeronauticos. Member AIAA.

†Assistant Professor of Aircraft Design, Department Vehiculos Aeroespaciales, Escuela Tecnica Superior de Ingenieros Aeronauticos.